A Markovian Approach Applied to Reliability Modeling of Bidirectional DC-DC Converters Used in PHEVs and Smart Grids

M. Khalilzadeh*, A. Fereidunian*(C.A.)

Abstract: In this paper, a stochastic approach is proposed for reliability assessment of bidirectional DC-DC converters, including the fault-tolerant ones. This type of converters can be used in a smart DC grid, feeding DC loads such as home appliances and plug-in hybrid electric vehicles (PHEVs). The reliability of bidirectional DC-DC converters is of such an importance, due to the key role of the expected increasingly utilization of DC grids in modern Smart Grid. Markov processes are suggested for reliability modeling and consequently calculating the expected effective lifetime of bidirectional converters. A three-leg bidirectional interleaved converter using data of Toyota Prius 2012 hybrid electric vehicle is used as a case study. Besides, the influence of environment and ambient temperature on converter lifetime is studied. The impact of modeling the reliability of the converter and adding reliability constraints on the technical design procedure of the converter is also investigated. In order to investigate the effect of leg increase on the lifetime of the converter, single leg to five-leg interleave DC-DC converters are studied considering economical aspect and the results are extrapolated for six and seven-leg converters. The proposed method could be generalized so that the number of legs and input and output capacitors could be an arbitrary number.

Keywords: Bidirectional converter, reliability, plug-in hybrid electrical vehicle (PHEV), DC Microgrid, Markov modeling, Smart Grid.

1. Introduction

The usage of power electronic devices in various applications has been increased significantly in recent years. Consequently, a number of papers has been dedicated recently to investigate the reliability of these devices [1-4]. In modern electrical grid, power electronic systems are considered as a vital part of the system. As an example, bidirectional DC-DC converters (BDC) play a major role in new plug-in electrical vehicles and their interaction with the electrical grid. Figure 1 shows a schematic of this interaction.

Due to the variable structure of power electronic converters, the analysis of their reliability is complicated in many cases. In [5, 6], DC-AC inverter reliability in electrical vehicles, particularly inverter part of the photovoltaic module has been studied. However, the mentioned inverter is not fault-tolerable. Markov modeling has been utilized in [7] to model the reliability of a fault tolerant active filter. In several papers, different topologies and control methods have been developed for DC-AC inverters and DC-DC converters, claiming that their proposed topology is superior in terms of reliability. Nevertheless, the reliability has not been quantitatively discussed. For instance in [8], a control method is proposed to improve the reliability of a matrix converter or in [9], an adaptive control method is introduced, which aims to boost the performance and the reliability of wind-turbine converters.
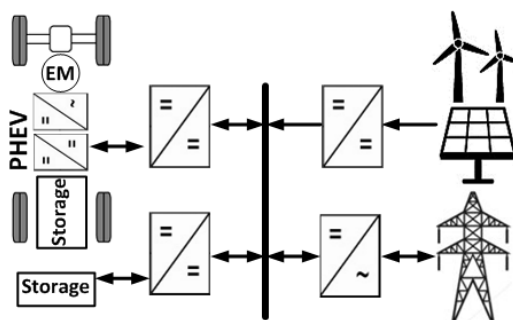

Fig. 1. Simple schematic of a DC grid in Smart Grid

Nevertheless, in both papers, quantitative reliability indices are not considered. The first step to compare the reliability of a circuit with the previous works is to determine numerical indices for that. Nonetheless, a few papers have evaluated them.

Some papers have investigated uni-directional DC-DC converters reliability. In [10], a comparison has been made between reliability of basic unidirectional DC-DC converters in photovoltaic applications. Reference [11] has compared a boost, buck-boost, back-to-back and matrix converter, to find the most reliable one in wind energy conversion system. In both of these references, the converters were uni-directional.

One of the most important types of dc-dc converters, which is used in a variety of applications, is the interleaved converter. The advantages of these converters have been studied in different papers [12-15]. Although the current split between different legs increases the lifetime of the devices, the drawback is that increasing number of parts in converter may result in decreasing its overall reliability. Hence, in applications in which the reliability is the first priority, the converter is designed to be fault tolerable in order to increase the reliability.

In [16], a three-leg unidirectional interleaved DC-DC converter of a PV module is studied in terms of reliability. Nevertheless, the effect of sensors and inductors and the photovoltaic cells is not considered in reliability calculations of the system. In [17], a photovoltaic module is studied, considering the effect of failure rate of the sensors and photovoltaic cells on reliability. In [18], the reliability indices of a unidirectional two-leg interleaved photovoltaic converter are discussed. In the two latter mentioned papers, the converter is not fault-tolerable and therefore reliability calculations are based on the assumption that all elements are in series. In [19], reliability evaluation of a boost interleaved converter is studied considering temperature effect. The environment effect on converter lifetime, economic aspects and its lifetime expectation were not discussed.

In all of these cases the converters were uni-directional. One important sort of converter is the bidirectional one, which is widely used in plug-in electric vehicles, smart homes, DC grids, aircrafts, and satellite power supplies. In the applications in which reliability is of high priority, these converters should be highly fault-tolerant. A reliability model is needed to be developed to evaluate the effective lifetime of these converters. Fault tolerant BDCs have rarely been investigated from the reliability point of view up to now, to the best of our knowledge. Since these converters have multi-state structures, Markov method could be used to model mean time to failure (MTTF) of these converters. This modeling allows the designers to consider reliability and MTTF of these converters as a technical factor. Since in vehicle and military applications the lifetime and reliability are of highest concerns, using

these factors could affect significantly the design procedure and number of elements used. This paper aims to propose an approach to model the reliability of BDCs especially the fault-tolerant interleaved ones. Furthermore, the MTTF of the converters is derived, based on the developed model. The present paper is organized as follows: In section 2, basic definitions are given and required indices are presented. Markov process and the proposed model of the BDC based on this process are expressed, and the circuit part of the system and its different topologies (based on switches) are introduced. Then the system is modeled from the reliability point of view using Markov process method in section 3. The reliability model derived in Section 3 is applied in section 4 to a 27kW fault-tolerant BDC and the simulation results, economic aspects and comparisons are discussed.

2. Method
2. 1. Stochastic Reliability Modeling

This sub-section provides the reader with the mathematics of stochastic reliability modeling. Reliability is the probability of a device performing its purpose adequately for the intended period of time under the operating conditions encountered [20]. Reliability function R(t) denotes the probability of proper functioning of the system in time interval [0, t], which should cover the warranty period that companies offer to customers [21].

The most important numerical indices to evaluate the reliability of power electronic equipment are: reliability function, failure rate, MTTF, and availability of the system. The reliability function can be represented as in (1) [1, 20-22]:

$$R(t) = e^{-\lambda t} \tag{1}$$

where "λ" denotes system (or component) failure rate. MTTF is the expected time of proper functioning of the system before failure occurrence. This index which plays a key role in this study is defined as (2) [1, 20-22]

$$MTTF = \int_0^\infty R(t)dt \tag{2}$$

Substituting (1) in (2) yields the below equation:

$$MTTF = \frac{1}{\lambda} \tag{3}$$

A system is described by its different states, and the transition between these states. A state diagram, known as "Markov Diagram", is a way to show all of the possible

sates and transitions between them. The state transition of a Markov diagram can be formulated as equation (4) [1, 20-22]:

$$P'(t) = P(t) \times A \tag{4}$$

where P(t) and A are the probability of system being in a specific state as a function of time "t" and transition rate between states matrices respectively. P' (t) is the derivative of the probabilities vector with respect to "t". Solving this matrix equation, one can calculate the probability of being in a specific state, as a function of the time "t". However, in this paper, only the limiting state or steady-state probabilities are of interest, which can easily be calculated by the following method [20-22].

First, stochastic transition probability matrix (STPM), which is an n×n matrix, is defined as below (n is the number of the states) [20, 22].

$$STPM = I_n + A \tag{5}$$

where "I_n" is n×n Identity matrix. This matrix presents the probabilities of making a transition from one state of the system to another. A method based on truncated probability matrix Q is used to calculate the MTTF of the system. For doing so, Q is calculated by removing the column and the row corresponding to the failure state – that is considered as an absorbing state– in STPM matrix. The matrix Q is determines the average time, i.e., MTTF, that would elapse before the system entered the failure state. Then, "M" which is an (n-1)×(n-1) matrix is calculated from the following equation:

$$M = [I_n - Q]^{-1} \tag{6}$$

Considering the state 1 as the starting state of the system, the MTTF of the system could be calculated by: (7) [20, 22]:

$$MTTF = \sum_{i=1}^{n-1} M(1, i) \tag{7}$$

The given mathematics in the sub-section is used for the reliability assessment in this paper.

2. 2. Reliability Assessment Methodology

Figure 2 shows a flowchart of the reliability assessment method. In this flowchart, bidirectional converters are cat-
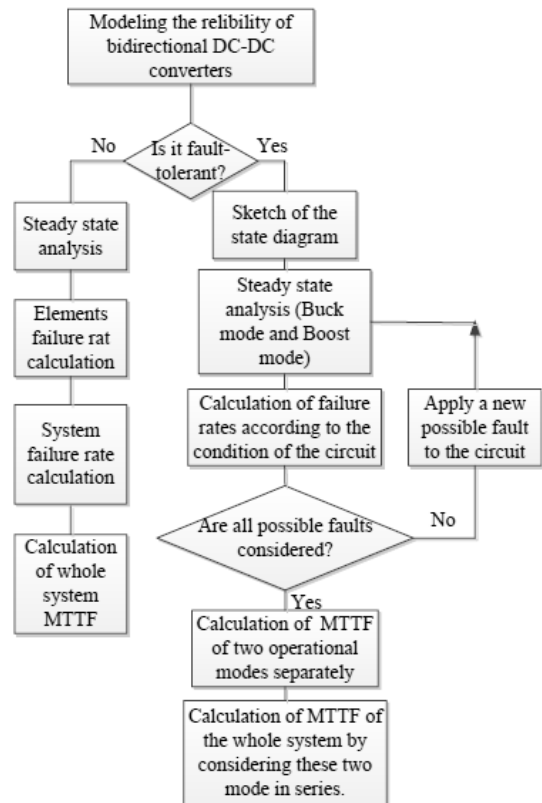

Fig. 2. Flowchart of the reliability assessment methodology.

egorized as fault tolerant and non-fault tolerant converters. In this paper, the main focus is on fault-tolerant converters. These converters have more operational states, since after fault, the switching configuration and consequently the topology will be changed. The proposed approach is also applicable to non-fault-tolerant converters.

3. Case Study and System Modeling
3. 1. Circuit Description

The application of interleaved bidirectional DC-DC converters (IBDC) in electrical vehicles has been studied in the literature, [23, 24]. However, the investigation of reliability of these converters and comparison of this feature for modern and conventional converters have not been studied in-depth before. The structure used in this paper is depicted in figure 3.

This converter is a fault-tolerant three-leg IBDC. One of the most vulnerable parts of a converter is the capacitor used in DC links [6, 21]. In highly reliable applications, the design is often based on redundancy; therefore, in this converter, two parallel capacitors are used in the output. Failure of one capacitor leads to a lower "capacity" which means higher voltage fluctuations. These fluctuations
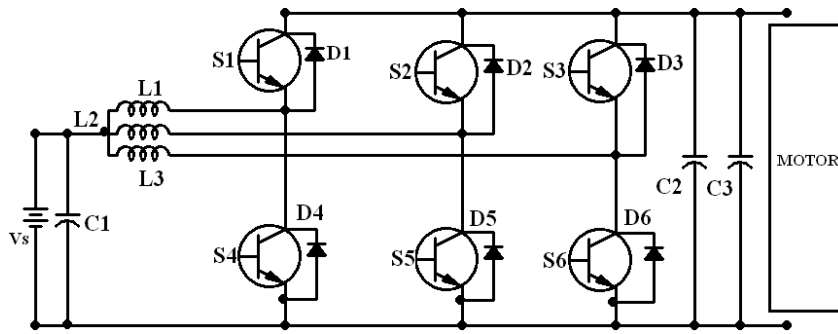
Fig. 3. Fault-tolerant bidirectional three-leg (phase) interleaved DC-DC converter

cause a change in failure rate of the remaining capacitor, which should be considered in calculations. Failure of a device in one leg causes removal of that leg, and the system provides the required power through remaining healthy legs. The assumption is that high reliability is a requirement, and consequently the system is designed in a way that the other legs can bear the total power. It should be noted that the design of the system and selection of the elements depends on the application for which the system is used. If the objective is to reduce the sizes of the elements, and the converter does not possess the fault tolerance feature, then failure of one leg means the failure of the system, because remaining legs could not tolerate and handle the whole power flow. In these applications, from the reliability point of view, all elements are in series, and the reliability is calculated from (8):

$$R(t) = \prod_{i=1}^{n} R_i \qquad (8)$$

where "n" is the number of elements. However, in high-reliability applications, like military applications or very important load centers, the elements should be selected in a way that failure of one leg causes the system to change its topology so that it could transmit the required power. Therefore, all elements could not be modeled in series, and a more sophisticated model is necessary.

In PHEVs, when the motor is in the acceleration mode, the power is transmitted from the battery to the motor. In this case, lower part switches will play the role in power transmission and the upper part switches are off. The result will be a "Boost Interleaved Converter" depicted in figure 4. In the braking mode, the power flow direction is reversed and the upper part switches are ON, and the resultant is a "Buck Interleaved Converter" shown in figure 5. Two mentioned topologies will be analyzed separately.

Correct operation of the whole system requires both topologies to be operated properly. Hence, from the reliability point of view, they could be considered in series to model the reliability of whole system, as shown in figure 6.

In high-voltage applications, utilization of IGBT switches is more common, because of its lower conduction voltage drop. Nevertheless, the failure rate of these kinds of switches is not mentioned in MIL-HDBK-217F [25] and [26], which are of the major literature in this field. In some papers, the existing information of MOSFET switches has been used to estimate the failure rate of IGBTs [27]. However, in this paper, a different approach
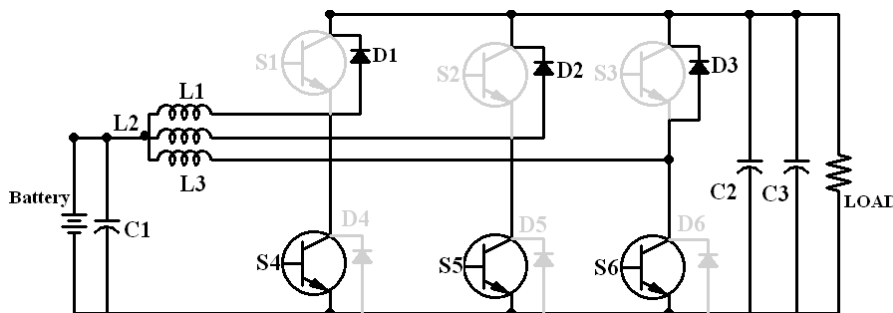

Fig. 4. Boost mode - supplying the motor from battery
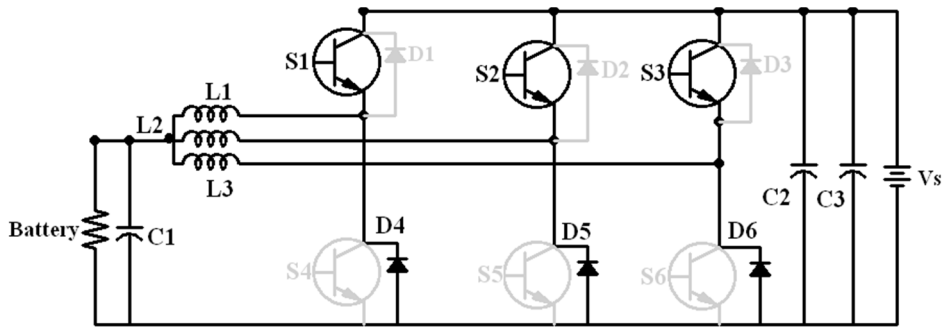(acceleration mode)

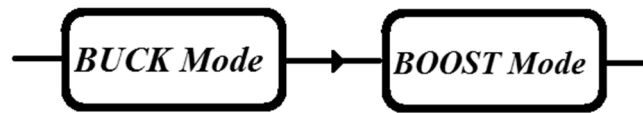**Fig. 5.** Buck mode - charging the battery
(braking mode)

Fig. 6. The model of the whole system from the reliability point of view

is employed. Since an IGBT could be modeled as a MOS-FET switch connected to a PNP BJT transistor [28], the proper functioning of the IGBT depends on the correct behavior of these two devices. Therefore, to calculate the reliability of an IGBT, these two items could be considered in series, which means the failure rate of an IGBT equals sum of the failure rate of the MOSFT switch and the BJT transistor as shown in (9,10) [20, 29].

$$\lambda_{Elements\ in\ series} = \sum_{i=1}^{n} \lambda_i \tag{9}$$

$$\lambda_{IGBT} = \lambda_{MOSFET} + \lambda_{BJT} \tag{10}$$

Two kinds of sensors, i.e., voltage sensor and current sensor, are used in the converter, and failure of them causes the control part of the system to operate incorrectly, which leads to the failure of the system. Besides, upper switches are packaged with an optocoupler, and their failure rate should be considered as well.

3. 2. Parts Failure Rates Calculation

In MIL-HDBK-217F [25] and [26], the failure rates of the elements are given according to a base value (λ_b) and some correction factors (π_x). These values are used in this paper to calculate the transition rate matrix and then MTTF of the system.

The failure rates of elements of the converter are given in (11)-(17) [25, 26]:

$$\lambda_{Diode} = \lambda_b.\pi_T.\pi_S.\pi_C.\pi_Q.\pi_E = \lambda_D \tag{11}$$

$$\lambda_C = \lambda_b.\pi_T.\pi_{SR}.\pi_C.\pi_V.\pi_Q.\pi_E \tag{12}$$

$$\lambda_{MOSFET} = \lambda_{bM}.\pi_{TM}.\pi_A.\pi_Q.\pi_E \tag{13}$$

$$\lambda_{BJT} = \lambda_{bB}.\pi_{TB}.\pi_A.\pi_Q.\pi_E.\pi_R \tag{14}$$

$$\lambda_{Optocoupler} = \lambda_b.\pi_T.\pi_S.\pi_Q.\pi_E \tag{15}$$

$$\lambda_{Inductor} = \lambda_b.\pi_T.\pi_Q.\pi_E = \lambda_{Ind.} \tag{16}$$

$$\lambda_{Sensor} = \lambda_b.\pi_T.\pi_P.\pi_S.\pi_Q.\pi_E \tag{17}$$

Table 1 shows the base values of failure rates and some correction factors. The definitions and formulations of the correction factors are given in [25, 26]. Base values are constant, however, some correction factors, .e.g., voltage stress and temperature, are needed to be changed according to the environment, operation condition, etc. When circuit topology are altered, these factors are recalculated based on the current, voltage ripple and temperature. As

Table 1. The circuit elements base failure rates, environment factors, and quality factors considered in this study

Circuit elements	$\lambda_b(\dfrac{\text{Failures}}{10^6\text{Hours}})$	π_E (GM)	π_Q
Diode	0.025	9	5.5
MOSFET	0.012	9	5.5
BJT	0.00074	9	5.5
Capacitor	0.00012	20	3
Opto-isolator	0.013	8	5.5
R_{sense}	0.0037	16	3
Inductor	0.00003	12	3

a result, failure rate of the element in the new circuit condition could be obtained.

The temperature of the junction (T_j) is a function of dissipated power in elements (P_S), case thermal resistance (R_{th}) and ambient temperature (T_a). It is calculated based on (18):

$$T_j = T_a + (\theta_{ca} + \theta_{jc})P_s = T_a + R_{th}.P_s \tag{18}$$

Neglecting the leakage current of switching devices in off state, P_s can be obtained for each semiconductor device as follows:

$$P_s = \frac{1}{T_s}\int_0^{T_s}(V_{off} + R_{on}i_{on}(t))i_{on}(t)dt \tag{19}$$

where R_{on} and i_{on} are the conducting-state resistance and conducted current of the element respectively and V_{off} is the reverse voltage drop.

3. 3. System Markov Modeling

The Markov method is used here to model the reliability of the system. Two different topologies, i.e., buck during charging the battery and boost during supplying the motor are used and analyzed separately and then they are considered in series to derive the reliability indices of the whole system, as shown in figure 6.

3. 3. 1. Modeling the Positive Acceleration State (Boost)

In the first topology, i.e., boost topology (figure 4), the system consists of 6 operation states and one failure state. The Markov diagram of this topology is shown in figure 7. Any failure in the switches, diodes and inductors causes the loss of one leg; therefore, the direction of state transition will be from left to right. In this case, loss of any leg, changes the current of the remaining legs, which alters their failure rate. On the other hand, failure of any capacitor in high-voltage side, leads to a transition state from

up to down. Loss of an output capacitor results in an increase in voltage ripple of the remaining capacitor, and its failure rate will increase. It means that some of the correction factors cannot be considered constant and should be calculated repeatedly during calculation process. As an example, failure rate of the elements in state 2 is different compared to their failure rates in state 1. The discrepancy between these rates, which could be calculated according to the simulation and voltage ripple, elements power, etc., is considered in the reliability calculations and MTTF. As mentioned before, the failure of every sensor means the failure of the system, i.e., transition to state 7. The state transition equations are coming hereafter.

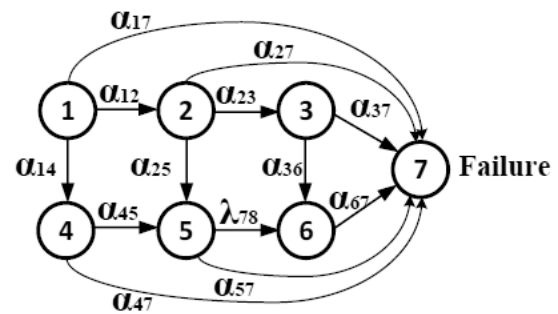$$\alpha_{23,56} = 2(\lambda_{D1} + \lambda_{IGBT1} + \lambda_{Ind.1}) \tag{20}$$

Fig. 7. Markov model of the boost mode

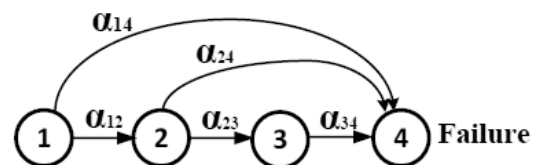**Fig. 8.** Markov model of the buck mode

$$\alpha_{37} = (\lambda_{D2} + \lambda_{IGBT2} + \lambda_{Ind.2} + 2\lambda_{sensor}) \quad (21)$$

where "λ_{xn}" shows the failure rate of element "x" after loss of "n" legs. For example, "λ_{D2}" represents the failure rate of diode D, when two legs are out. Note that the effect of increase of conducting current is considered in this calculation. Moreover, "α_{ij}" represents the state transition from state "i" to state "j".

$$\alpha_{12,45} = 3(\lambda_{D0} + \lambda_{IGBT0} + \lambda_{Ind.0}) \quad (22)$$

$$\alpha_{14} = 2\lambda_{C00} \quad (23)$$

$$\alpha_{25} = 2\lambda_{C10} \quad (24)$$

$$\alpha_{36} = 2\lambda_{C20} \quad (25)$$

$$\alpha_{47} = \lambda_{C01} + 2\lambda_{sensor} \quad (26)$$

$$\alpha_{57} = \lambda_{C11} + 2\lambda_{sensor} \quad (27)$$

where "λ_{Cuv}" corresponds to the failure rate of a capacitor after loss of "u" legs and "v" capacitors.

$$\alpha_{67} = \lambda_{C21} + \lambda_{D2} + \lambda_{IGBT2} + \lambda_{Ind.2} + 2\lambda_{sensor} \quad (28)$$

$$\alpha_{17,27,47,57} = 2\lambda_{sensor} \quad (29)$$

3. 3. 2. Charging Mode Modeling (Buck)

The topology of the circuit during battery charging is shown in figure 4. In this mode, all of three legs transmit the power, but only one capacitor is connected to LV part, which means there will be no vertical transition in the state diagram. The Markov diagram is depicted in figure 8. The equations of all state transitions could be written in a same way of boost mode.

4. Numerical results and discussions
4. 1. Simulation Results

To calculate failure rates and MTTF numerically and to verify the analysis, a three-leg fault-tolerant IBDC have been simulated in MATLAB Simulink. The components which are available in Simulink library are used to simulate the elements, and data mentioned in datasheets, i.e., nominal and parasitic values, are entered as the element rated values. The design parameters of the system, i.e., input and output voltage, nominal power and switching frequency, are based on the real data of Toyota PRIUS 2010 hybrid electrical vehicle [30]. The specifications and parameters used for the simulation are given in Table 2.

Two modes of operation i.e., boost mode and buck mode are simulated separately. The simulation has been done for different kinds of failures in different states of operation. For each of them, the failure rates of all elements are calculated according to equations (11-17), conditions of the simulated circuit and its elements voltage, current, and power equations. Figure 9 shows simulated output voltage of the converter in boost mode, after and before occurrence of fault due to loss of one capacitor.

Table 2. Specification and parameters of the model

| Parameter	Value/Part number
Self-inductance	0.8 mH
Mutual inductance	0.7 mH
Winding resistance of each phase	0.07 Ω
Capacitor HV	$2 \times 47\mu F$
Capacitor LV	$47\mu F$
Battery (Fully charged)	201 V
V_{dc}	650 V
Forward voltage drop of diode	1.8V
Switching frequency	25 kHz
Nominal power	27 kW
HV capacitor voltage rating	800V
LV capacitor voltage rating	250V
IGBT	2MBI150U4A-120
Diode junction-case thermal resistance	0.28°C/W
IGBT junction-case thermal resistance	0.17°C/W
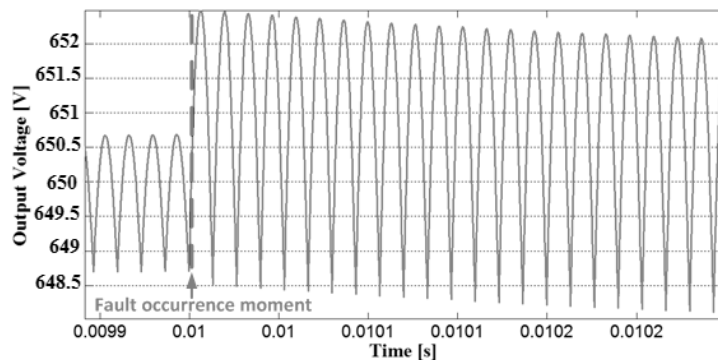
Fig. 9. Output voltage of the converter in boost mode before and after one output capacitor failure

The results have been summarized in Tables 3 and 4 for boost and buck mode, respectively. Then, from equations (20-29) and same equations for buck mode, Markov diagram transition rates, i.e., α_{ij}, will be obtained. Based on these rates, MTTF of the buck and boost mode could be found separately by using equation (7). With MTTF calculated, the failure rates of two modes of operation will be calculated from (3), and by using (9), equation (30) could be derived for calculating the failure rate of the whole system:

$$\lambda_{Total} = \lambda_{buck\ mode} + \lambda_{boost\ mode} \qquad (30)$$

Finally, the MTTF of the total system is calculated according to (3).

In calculation of failure rates, the biggest among the correction factors is the Environment factor which plays the most important role. Figure 10 shows the MTTF For different environments. As shown, the difference between lab condition, i.e., "GB" and mobile condition causes a significant difference between their MTTFs. In some papers, such as [16], it is assumed that the environment is stable, clean, and fixed e.g., the lab environment. Therefore the Environment factor is taken equal to 1. However, for PHEV application, the vehicle is often used in different conditions, and according to [25], Environment factor

Table 3. Calculation and simulation results for the failure rate of circuit elements in "Boost" mode

	λ for Other components [failure/10^{-6}h]			**λ for Capacitor** [failure/10^{-6}h]					
Failure mode	**0**	**1**	**2**	**00**	**10**	**20**	**01**	**11**	**21**
Diode	1.14345	1.33403	2.38219						
IGBT	9.2233	10.1761	18.5044						
Capacitor				0.1066	0.1082	0.1161	0.1080	0.1149	0.1225
Inductor	0.00119	0.00124	0.0013						
Sensor	0.03321	0.03472	0.0362						

Table 4. Calculation and simulation results for the failure of circuit elements in "Buck" mode

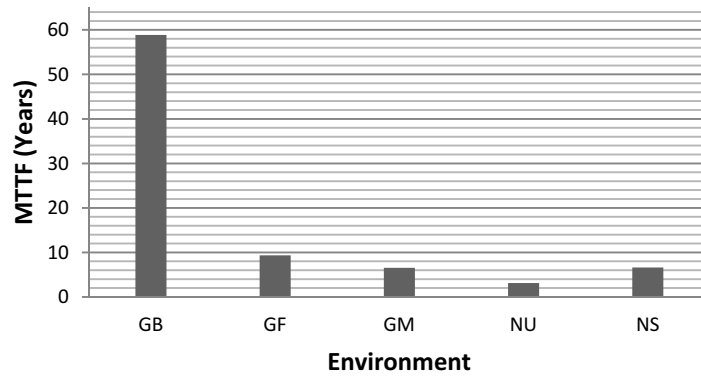|	**λ [failure/10^{-6}h]**		
Failure mode	**0**	**1**	**2**
Diode	1.43884	1.71518	3.14449
IGBT	11.54521	13.15042	15.45206
Capacitor	0.10213	0.10235	0.10297
Inductor	0.00119	0.00124	0.00130
Sensor	0. 03321	0.03472	0.03623
Optocoupler	0.68640	0.68640	0.68640

Fig. 10. Effect of operation environment on MTTF; "GB" = Ground, Benign; "GF"= Ground, Fixed; "GM"=Ground, Mobile; "NU"= Naval, Unsheltered; and "NS"= Naval, Sheltered.

should be considered "GM" (Ground, mobile) [25], thus simulating a more realistic environment. In this case, for each element, Environment factor will be selected from Table 1. It is observed that the failure rate of the circuit elements is bigger compared to the "GB". Besides, as could be seen in figure 10, the difference between these rates in "GB" environment and "GM" environment causes a significant difference in MTTF, i.e., up to nine times. Also the figure shows that if the converter is used in fixed-location applications with normal maintenance (GF), e.g., energy part of smart homes, the converter will be expected to last about 43% longer than when it is used in a PHEV. For the calculated MTTF, the assumption is that the automobile (and consequently the converter) is used continuously. However, in reality, the automobiles are used much less frequently and therefore their lifetime will be higher than the given results.

4. 2. Sensitivity Analysis
4. 2. 1. Capacitor Value Analysis

As mentioned before, one of the most important advantages of reliability assessment for converters is including technical constraints into the design and selection of circuit elements. The new constraints optimize the system from both performance and reliability point of view. To clarify the issue, an example is given here.

Selecting an appropriate value for the high-voltage capacitors is an important part of the design. Neglecting output capacitors equivalent series resistance (ESR), one can obtain the following equation for the output voltage ripple in boosting mode:

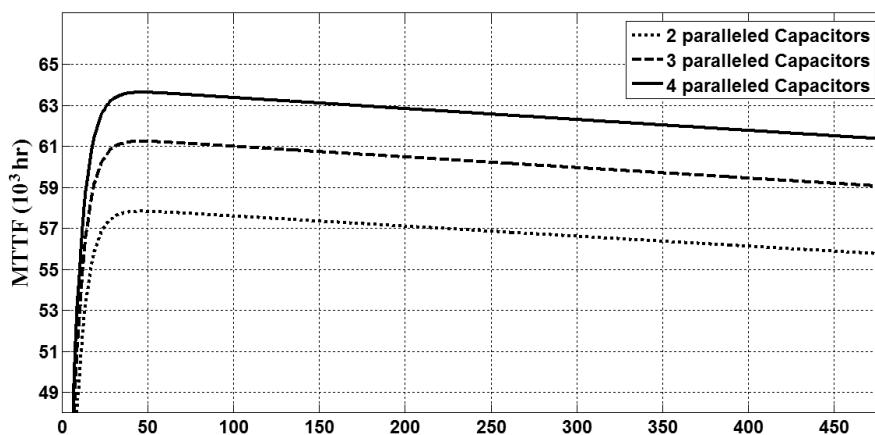$$\Delta V_{out} = (I_{out}.D)/(f_s.C_{out}) \tag{31}$$

Fig. 11. Effect of output capacitors value and arrangement on the MTTF of the converter

where "D" and "f_s" are switch duty cycle and switching frequency, respectively. According to (31), to reduce output voltage ripple, thus increasing the life time of the capacitors by reducing π_v in (12), the capacitance should be increased. On the other hand, increasing the capacitance itself reduces the life time via increasing π_C coefficient. Therefore, a compromise should be made between voltage ripple and reliability of the system.

Figure 11 shows the value of final MTTF of the system based on different high-voltage capacitor values. As it could be seen, the MTTF curves have a maximum values and after that, they begin to decrease. Another important point is that increasing the number of paralleled capacitors results in an increase in MTTF. Therefore, the best approach to obtain a desired voltage ripple is to increase the capacitance through paralleling capacitors. It causes not only a rise in MTTF, but also reduction in ESR and losses of the converter.

4. 2. 2. Redundancy Analysis

Dependence of the MTTF to the number of capacitors and other circuit elements redundancy is not linear. To investigate this issue, a comparison has been made between single-leg (conventional) to five-leg interleaved DC-DC converters with similar parameters in terms of MTTF. Besides, in order to include economic aspects, the authors utilize an index called "cost factor", which is introduced by [31, 32] as:

$$CF = \frac{\sum k(\text{Fault−tolerant converter})}{\sum k(\text{Conventional converter})} \quad (32)$$

This is a normalized index for cost comparison between fault-tolerant interleaved topologies. Table 5 summarizes cost weightings used for CF calculation.

Table 5. Cost weighting coefficients [32]

components	k
Capacitor (input)	1.5
Capacitor (Output)	1.5
Inductor	3
Gate drive	0.3
IGBT	2

Results are discussed in table 6 and figure 12. Note that the curve points for six and seven legs converters are extrapolated, and are shown by dashed lines. All MTTFs are normalized based on MTTF of conventional dc-dc converter. As it could be seen, the MTTF of five-leg interleaved converter is about 3.165 times bigger compared to the conventional converter. As said before, redundancy in legs does not linearly increase MTTF, i.e., higher number of legs leads to a slower rate of MTTF increment. It could be seen that as the number of legs rises, the cost (CF) increases almost linearly, but the MTTF increment rate reduces. It leads to the divergence of the two curves when the number of legs is relatively high. When the number of legs is too high, the amount of life time increment made by adding one more leg is not justifiable in terms of price. Therefore a compromise between the number of legs and the production cost should be made. Nevertheless, in applications where high reliability is needed, it is justifiable. It should be noted that for two and three-leg converters, the normalized cost and MTTF are close, which makes them good candidate for typical applications.
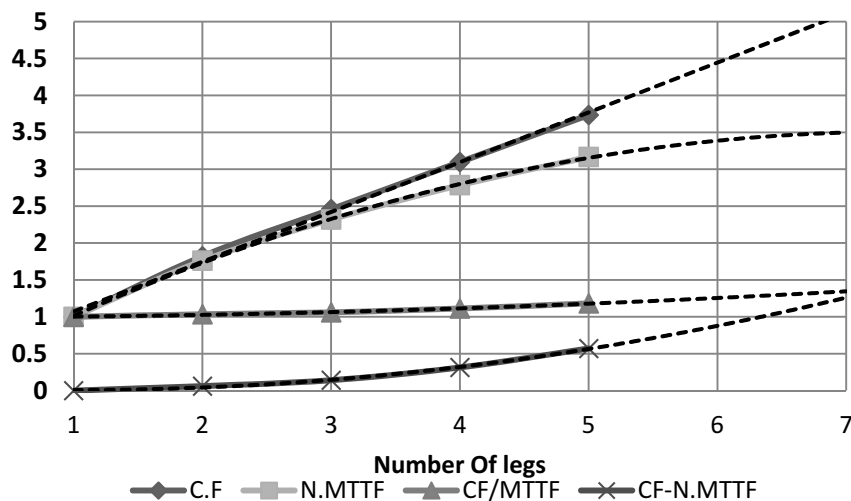

Fig. 12. Effect of leg increase in cost and MTTF of the DC-DC converter

Table 6. Summarized results of CF and MTTF

Number of legs	1-leg	2-leg	3-leg	4-leg	5-leg
Buck mode MTTF	5.8664	9.4839	12.2168	14.37	16.2334
Boost mode MTTF	5.4146	10.372	14.0116	17.2433	19.76
Whole system MTTF	2.8157	4.9540	6.5264	7.8380	8.9119
Normalized MTTF*	1	1.7594	2.3179	2.7837	3.1651

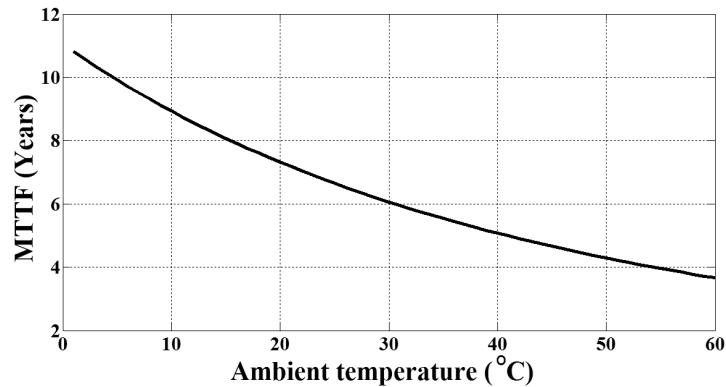*Normalized MTTF= (Whole system MTTF)/ (1-leg converter MTTF)

Fig. 13. Effect of operation temperature on converter MTTF

4. 2. 3. Temperature Effect Analysis

In the results presented before, the assumption was that the ambient temperature is 25℃; however, in reality, it could be higher. The ambient temperature affects the junction temperature based on equation (18) and the failure rate of the elements through π_T. It means that a change in the temperature could change the MTTF of the whole system. Hence, studying this effect on the converter lifetime is necessary. To do so, the ambient temperature will be raised from a small positive value up to 60℃, and the simulation will run for each temperature rise step, and MTTF for each temperature step will be calculated. The results are shown in figure 13. It is observed that MTTF of a converter working in ambient temperature of 50℃ will be 0.66 times compared to a converter working in ambient temperature of 25℃. Hence, existence of a proper cooling system e.g. liquid-cooling system is necessary in hot temperatures.

5. Conclusion

In this paper, a fault-tolerant IBDC was studied in terms of its reliability using a stochastic Markovian approach. Studying the reliability indices helps PHEV manufacturers to have a more accurate estimation about warranty period they can offer to the customers. The converter was modeled by the Makov-process and then the MTTF index was calculated. The proposed method could be generalized so that the number of legs and input and output capacitors could be an arbitrary number. Two to five-leg interleaved and conventional converters were compared, then it was observed that rising the number of leg redundancies increases the reliability of the system such that the lifetime of five-leg systems was 3.165 times compared to conventional converters. However, the increment is not linear and the rate of increment of MTTF reduces as the number of legs increases, i.e., showing a saturation behavior. To investigate the economic aspects of leg increment in BDCs, a factor named "Cost factor" was used. It was concluded that the increase in the number of legs would result in the divergence of MTTF and cost factor curves. In other words, the rate of increase is not the same in these two curves. The effect of reliability constrains on the converter design and element values was also investigated. Environment and temperature effects on MTTF were studied and it was seen that an increase in temperature results in the reduction of lifetime of the converter. As an example, the lifetime of a converter working in ambient temperature of 50℃, will be 0.66 times of a

converter working in ambient temperature of 25℃. The proposed method is promising and could be used for modeling any IBDCs with any number of legs in Smart Grid.

References

[1]   F. Richardeau and T. T. L. Pham, "*Reliability Calculation of Multilevel Converters: Theory and Applications,*" IEEE Transactions on Industrial Electronics, vol. 60, pp. 4225-4233, 2013.

[2]   C. W. Zhang, T. Zhang, N. Chen, and T. Jin, "*Reliability modeling and analysis for a novel design of modular converter system of wind turbines,*" Reliability Engineering & System Safety, vol. 111, pp. 86-94, 2013.

[3]   H. Wang and F. Blaabjerg, "*Reliability of capacitors for DC-link applications in power electronic converters—An overview,*" IEEE Transactions on Industry Applications, vol. 50, pp. 3569-3578, 2014.

[4]   K. Ma, M. Liserre, F. Blaabjerg, and T. Kerekes, "*Thermal Loading and Lifetime Estimation for Power Device Considering Mission Profiles in Wind Power Converter,*" IEEE Transactions on Power Electronics, vol. 30, pp. 590-602, 2015.

[5]   D. Hirschmann, D. Tissen, S. Schroder, and R. W. D. Doncker, "*Reliability Prediction for Inverters in Hybrid Electrical Vehicles*," IEEE Transactions on Power Electronics, vol. 22, pp. 2511-2517, 2007.

[6]   A. Ristow, M. Begovic, A. Pregelj, and A. Rohatgi, "*Development of a Methodology for Improving Photovoltaic Inverter Reliability*," IEEE Transactions on Industrial Electronics, vol. 55, pp. 2581-2592, 2008.

[7]   P. Poure, P. Weber, D. Theilliol, and S. Saadate, "*Fault-tolerant Power Electronic Converters: Reliability Analysis of Active Power Filter,*" in 2007 IEEE International Symposium on Industrial Electronics, 2007, pp. 3174-3179.

[8]   K. Nguyen-Duy, T. H. Liu, D. F. Chen, and J. Y. Hung, "*Improvement of Matrix Converter Drive Reliability by Online Fault Detection and a Fault-Tolerant Switching Strategy,*" IEEE Transactions on Industrial Electronics, vol. 59, pp. 244-256, 2012.

[9]   I. Trintis, S. Munk-Nielsen, F. Abrahamsen, and P. B. Thoegersen, "*Efficiency and reliability improvement in wind turbine converters by grid converter adaptive control,*" in 2013 15th European Conference on Power Electronics and Applications (EPE), 2013, pp. 1-9.

[10]   G. Graditi, D. Colonnese, and N. Femia, "*Efficiency and reliability comparison of DC-DC converters for single phase grid connected photovoltaic inverters,*" in SPEEDAM 2010, 2010, pp. 140-147.

[11]   M. Arifujjaman, "*Reliability comparison of power electronic converters for grid-connected 1.5 kW wind energy conversion system,*" Renewable energy, vol. 57, pp. 348-357, 2013.

[12]   O. Hegazy, J. V. Mierlo, and P. Lataire, "*Analysis, Modeling, and Implementation of a Multidevice Interleaved DC/DC Converter for Fuel Cell Hybrid Electric Vehicles,*" IEEE Transactions on Power Electronics, vol. 27, pp. 4445-4458, 2012.

[13]   P.-W. Lee, Y.-S. Lee, D. K. Cheng, and X.-C. Liu, "*Steady-state analysis of an interleaved boost converter with coupled inductors,*" IEEE Transactions on Industrial Electronics, vol. 47, pp. 787-795, 2000.

[14]   R. Giral, L. Martinez-Salamero, and S. Singer, "*Interleaved converters operation based on CMC,*" IEEE Transactions on Power Electronics, vol. 14, pp. 643-652, 1999.

[15]   X. Zhou, P. Xu, and F. C. Lee, "*A novel current-sharing control technique for low-voltage high-current voltage regulator module applications,*" IEEE Transactions on Power Electronics, vol. 15, pp. 1153-1162, 2000.

[16]   S. V. Dhople, A. Davoudi, A. D. Domínguez-García, and P. L. Chapman, "*A unified approach to reliability assessment of multiphase DC–DC converters in photovoltaic energy conversion systems,*" IEEE Transactions on Power Electronics, vol. 27, pp. 739-751, 2012.

[17]   A. M. Bazzi, K. A. Kim, B. B. Johnson, P. T. Krein, and A. Dominguez-García, "*Fault impacts on solar power unit reliability,*" in Applied Power Electronics Conference and Exposition (APEC), 2011 Twenty-Sixth Annual IEEE, 2011, pp. 1223-1231.

[18]   H. Calleja, F. Chan, and I. Uribe, "*Reliability-oriented assessment of a Dc/Dc converter for photovoltaic applications,*" in Power Electronics Specialists Conference, 2007. PESC 2007. IEEE, 2007, pp. 1522-1527.

[19]   A. Khosroshahi, M. Abapour, and M. Sabahi, "*Reliability evaluation of conventional and interleaved DC–DC boost converters,*" IEEE Transactions on Power Electronics, vol. 30, pp. 5821-5828, 2015.

[20]   R.Billinton, and R. N.Allan, "*Reliability Evaluation of Engineering Systems: Concepts and Techniques*", 2nd ed., New York and London: Plenum Press, 1992.

[21]   Y. Song and B. Wang, "*Survey on reliability of power electronic systems,*" IEEE Transactions on Power Electronics, vol. 28, pp. 591-604, 2013.

[22]   M. Rausand, and A. Høyland, "*System Reliability Theory: Models, Statistical Methods, and Applications*", 2nd Edition, New York, USA: Wiley-Interscience, 2003.

[23]   L. Ni, D. J. Patterson, and J. L. Hudgins, "*High*

power current sensorless bidirectional 16-phase interleaved DC-DC converter for hybrid vehicle application," IEEE Transactions on Power electronics, vol. 27, pp. 1141-1151, 2012.

[24] A. Ostadrahimi and A. Radan, "*Utilization of interleaved converter to improve battery performance in electric and electrical hybrid vehicles,*" in Power Electronics, Drive Systems and Technologies Conference (PEDSTC), 2014 5th, 2014, pp. 624-628.

[25] MIL-HDBK-217F—Military Handbook for Reliability Prediction of Electronic Equipment: Department of Defense, Washington, DC, Jan. 1990.

[26] W. Denson, D. Nicholls, P. Lein, R. Wisniewski, and P. Wagner, Handbook of 217Plus™ Reliability Prediction Models, 2nd Edn: Quanterion Solutions Incorporated, NY,USA, 2015.

[27] Y. Song and B. Wang, "*A hybrid electric vehicle powertrain with fault-tolerant capability,*" in Applied Power Electronics Conference and Exposition (APEC), 2012 Twenty-Seventh Annual IEEE, 2012, pp. 951-956.

[28] R. W. Erikson and D. Maksimovic, "*Fundamentals of power electronics: Kluwer academic*", 2001.

[29] E. Sutrisno, "*Fault detection and prognostics of insulated gate bipolar transistor (IGBT) using a k-nearest neighbor classification algorithm,*" 2013.

[30] Burress, T. A., Campbell, S. L., Coomer, C. L., Auers, C. W., Wereszczak, A. A., Cunningham, J. P., Mariliano, L. D., Seiber, L. E. and Lin, H. T. "*Evaluation of the 2010 TOYOTA PRIUS hybrid synergy drive system*", Report ORNL/TM-2010/253, Oak Ridge National Laboratory, UT-Battelle, LLC, , Oak Ridge, Tennessee, USA, 2011.

[31] M. Naidu, S. Gopalakrishnan, and T. W. Nehl, "*Fault-tolerant permanent magnet motor drive topologies for automotive x-by-wire systems,*" IEEE Transactions on Industry Applications, vol. 46, pp. 841-848, 2010.

[32] M. Boettcher, J. Reese, and F. W. Fuchs, "*Reliability comparison of fault-tolerant 3L-NPC based converter topologies for application in wind turbine systems,*" in Industrial Electronics Society, IECON 2013-39th Annual Conference of the IEEE, 2013, pp. 1223-1229.

spectively. His research interests include power electronic converters, reliability in power electronics, renewable energy, and electric motor drives.

Alireza Fereidunian is an Assistant Professor at the K. N. Toosi University of Technology, Tehran, Iran. He received his BS from IUST in 1994, and PhD and MSc from University of Tehran, in 2009 and 1997, where he is a Post-Doctoral Research Associate now. Alireza has been working as an electrical and automation engineer in energy distribution and industrial automation sectors, as well as working as a research scientist at Imperial College London and Aalto University. His research interests include Smart Grid, high-reliability energy distribution systems (automation and asset management), smart home, and application of data analytics to power systems. Moreover, he works in complex systems, systems reliability and human-automation interactions areas. He has developed essential ideas on Adaptive Autonomy Expert System (AAES) and Healer Reinforcement for Self-Healing in Smart Grid. Dr Fereidunian is a member of IEEE (PES), INCOSE and ISOSG.

Mohammad Khalilzadeh is a PhD Student in the University of Tehran, Tehran, Iran. He received his M.Sc. and B.Sc. in Electrical Engineering from K. N. Toosi University of Technology and the University of Tehran in 2012 and 2014 re-